Synthesis and Characterization of Luminescent Polyfluorenes Incorporating Side-Chain-Tethered Polyhedral Oligomeric Silsesquioxane Units

Chia-Hung Chou, So-Lin Hsu, K. Dinakaran, Mao-Yuan Chiu, and Kung-Hwa Wei*

Department of Materials Science and Engineering, National Chiao Tung University, Hsinchu, Taiwan 30049 R.O.C.

Received October 4, 2004; Revised Manuscript Received November 8, 2004

ABSTRACT: Using Suzuki polycondensation, we have synthesized polyhedral silsesquioxane-tethered polyfluorene copolymers, poly(9,9′-dioctylfluorene-*co*-9,9′-bis[4-(*N*,*N*-dipolysilsesquioxane)aminophenyl]-fluorene) (**PFO—POSS**), that have well-defined architectures. This particular **PFO—POSS** molecular architecture increases the quantum yield of polyfluorene significantly by reducing the degree of interchain aggregation; in addition, these copolymers exhibit a purer and stronger blue light by preventing the formation of keto defects.

Introduction

Semiconducting polymers have been studied extensively for their potential applications in electroluminescent displays,[1] solar cells,[2] and thin film organic transistors.[3] One of the most promising conjugated polymers is polyfluorene, which has been applied widely for its characteristic of emitting blue light.[4−7] Polyfluorenes may be functionalized readily by modifying the C-9 position of the fluorene monomer; such modification can, for instance, provide good solubility in common organic solvents that allows further processing. In the solid state, polyfluorene and its derivatives exhibit adequate photoluminescence (PL) and electroluminescence (EL) efficiencies.[8−10] The application of polyfluorenes in light emitting diodes, however, has been hampered by the appearance of green electroluminescence (ca. 530 nm) in addition to the desired peak at 425 nm; this green electroluminescence has been attributed to either intermolecular interactions, which lead to the formation of aggregates,[11−17] or to the presence of emissive keto defect sites that arise as a result of thermo- or electro-oxidative degradation of the polyfluorene backbone.[18a,b] A detailed discussion of this phenomenon has been presented elsewhere.[18c] As a result, the expected blue emission from polyfluorene becomes an undesired blue-green color in LED applications.

Several approaches have been adopted to reduce the formation of aggregation or keto defect in polyfluorenes, including the introduction of bulky side chains, using cross-linked structures, improving the oxidative stability of pendant groups or chain ends,[15] and limiting chain mobility by blending it with a high-T_g polymer.[17] One of the most recent approaches involves incorporation of polyhedral oligomeric silsesquioxane (**POSS**) into the conjugated polymer. The first such study was undertaken by attaching **POSS** covalently to the chain ends of poly(2-methoxy-5-[2-ethylhexyloxy]-1,4-phenylenevinylene) (**MEHPPV**) and poly(9,9′-dioctylfluorene) (**PFO**), which resulted in enhanced thermal stability of the devices prepared from these modified polymers.[15] The density of the polymer chain ends, however, decreases as the molecular weight of the polymer increases, which limits the amount of **POSS** that can be attached (ca. 1.2%). Another study involved a synthesis of a bridged polyfluorene copolymer by using fluorene tetrabromide monomers featuring a siloxane bridge. The thermal stability of a device made from this siloxane-bridged polyfluorene appears to be better than that prepared from pure **PFO**.[18d] A third related study involved attaching polyfluorene to the functionalized vertexes on the cubic polyhedral silsesquioxane core units to form starlike structures; these polymers possessed improved thermal and optoelectronic characteristics. The amount of **POSS** content in the polyfluorene was ca. 3.8%.[18e] The enhanced electroluminescence characteristics in these polyfluorenes have been attributed to **POSS** imparting a reduction in either the degree of aggregation and excimer formation or the number of keto defects. The molecular architecture that polyfluorene possessed in the latter two studies cannot be defined easily. Previously, we synthesized a polyimide-side-chain-tethered **POSS** as an approach to lowering its dielectric constant.[19a] In this present study, we took a copolymer approach by synthesizing polyfluorene-tethered **POSS** in a well-defined architecture. To the best of our knowledge, the introduction of an inorganic side group, such as **POSS**, into the C-9 position of polyfluorene has not been explored previously. We believe that by developing a **POSS**/polyfluorene copolymer having well-defined architecture we will be able to tailor its luminescence properties more precisely by modifying the molecular structure. In this paper, we report the synthesis and characterization of fluorene-based random copolymers featuring tethered polyhedral oligomeric silsesquioxanes (**POSS**) units.

Scheme 1 displays the synthetic procedure we used to prepare the **POSS—dibromide** monomer (**D-POSS—diAF**), in which cyclopentyl-**POSS** was covalently bonded to the C-9 carbon atom of the fluorene unit through a 4-aminophenyl spacer. We used **POSS—dibromide** as a comonomer, which, together with 2,7-dibromo-9,9′-dioctylfluorenone (**5**), were reacted with 2,7-bis(4,4,5,5-tetramethyl-1,3,2-dioxaborolan-2-yl)fluorene (**6**) through Suzuki coupling followed by end capping. Scheme 2 presents the complete synthetic

* Corresponding author. Telephone: 886-35-731871. Fax: 886-35-724727. E-mail: khwei@cc.nctu.edu.tw.

10.1021/ma0479520 CCC: $30.25
Published on Web 01/13/2005

Scheme 1. Synthesis of D-POSS−diAF (4)[a]

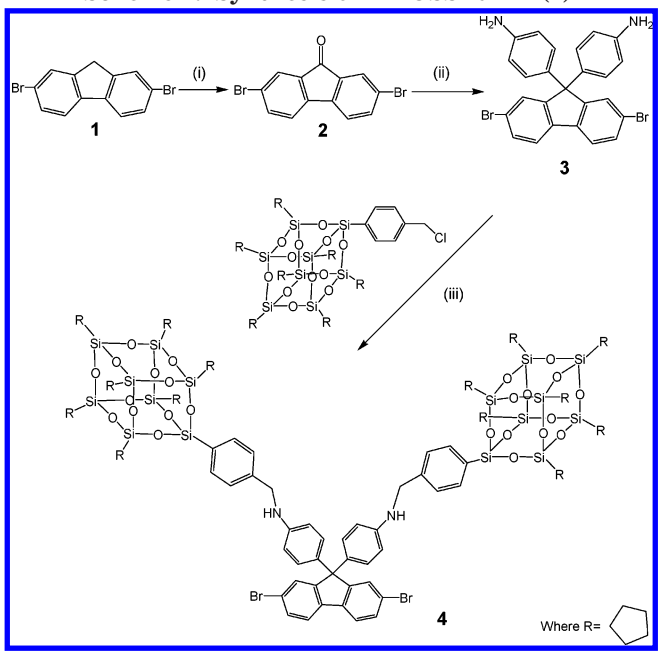

[a] (i) CrO_3, acetic anhydride, HCl_{aq}. (ii) aniline, aniline hydrochloride. (iii) K_2CO_3, KI, DMF/THF (5:4).

procedure for the preparation of **POSS**-tethered polyfluorene. The extended 9,9′-bis(4-aminophenyl)fluorenyl core, which is readily accessible, offers the following additional advantages: (1) Direct attachment of the benzyl groups of **POSS** to the C-9 carbon atom of the fluorene unit is avoided; such benzyl linkages are potentially susceptible to photooxidation, which may cause degradation and failure of the polymer LEDs.[19b,20] (2) The introduction of the 4-aminophenyl spacer reduces the steric hindrance imposed by **POSS**.[21] The insertion of a rigid phenylene spacer between the **POSS** side chain and the polymer backbone may lead to a shielding effect on the polyfluorene main chain, while leaving the reaction sites of the macromonomer accessible for the palladium-catalyzed polymerization reaction. (3) Through this copolymerization approach, the amount of **POSS** incorporated into the polyfluorene may be tuned by controlling the amount of **POSS—dibromide** monomer used in the polymerization.

Experimental Section

Materials. 2,7-Dibromo-9,9′-dioctylfluorenone (**5**),[21] 2,7-bis-(4,4,5,5-tetramethyl-1,3,2-dioxaborolan-2-yl)fluorene (**6**),[22] and the chlorobenzylcyclopentyl-**POSS**[23] were synthesized according to literature procedures. THF was distilled under nitrogen from sodium benzophenone ketyl; other solvents were dried using standard procedures. All other reagents were used as received from commercial sources unless otherwise stated.

Chlorobenzylcyclopentyl—POSS. ^{1}H NMR (300 MHz, $CDCl_3$): δ 7.64 (d, J = 8.1 Hz, 2H), 7.37 (d, J = 8.1 Hz, 2H), 4.57 (s, 2H), 2.26−1.21 (m, 56H), 1.16−0.81 (m, 7H) ppm. ^{29}Si NMR (600 MHz, THF): δ −67.8, −68.2, −79.6 ppm.

Synthesis of 9,9′-Bis(4-aminophenyl)-2,7-dibromofluorene (3). A mixture of 2,7-dibromo-9-fluorenone (**2**) (3.0 g, 8.88 mmol), aniline (4.0 g, 4.30 mmol), and aniline hydrochloride (1.15 g, 8.88 mmol) was heated at 150 °C under nitrogen for 6 h. The reaction mixture was then slowly added into water (150 mL) and extracted with ethyl acetate (3 × 50 mL). The combined extracts were dried ($MgSO_4$), the solvent was evaporated, and the residue was purified by column chromatography (hexane/ethyl acetate, 4:1) to afford **3** (3.23 g, 72%). ^{1}H NMR ($CDCl_3$): δ 7.52 (d, J = 8.1 Hz, 2H), 7.44 (4H), 6.90 (d, J = 8.1 Hz, 4H), 6.53 (d, J = 8.1 Hz, 4H), 3.58 (s, 4H) ppm. Anal. Calcd for $C_{25}H_{18}Br_2N_2$: C, 59.31; H, 3.58; N, 5.53. Found: C, 59.38; H, 3.62; N, 5.47.

Synthesis of 9,9′-Bis[4-(*N*,*N*-dipolysilsesquioxane)aminophenyl]fluorene (D-POSS-diAF) (4). 9,9-Bis(4-aminophenyl)-2,7-dibromofluorene (200 mg, 0.395 mmol) was stirred with K_2CO_3 (764 mg, 5.53 mmol) and KI (262 mg, 1.58 mmol) in DMF (5 mL) and THF (4 mL) at room temperature for 1 h. A small amount of **Cl—POSS** (888 mg, 0.832 mmol) was added and then the whole mixture was heated at 70 °C for 3 h. The reaction mixture was then slowly poured into water (150 mL) and extracted with chloroform (3 × 30 mL). The combined extracts were dried ($MgSO_4$), the solvents were evaporated, and the residue was purified by column chromatography (hexane/ chloroform, 1:10) to afford **4** (0.69 g, 68%). ^{1}H NMR ($CDCl_3$): δ 7.62−7.63 (m, 14H), 7.01−6.84 (m, 8H), 4.81 (s, 2H), 4.27 (s, 4H), 2.06−1.18 (m, 112H), 1.14−0.79 (m, 14H) ppm. Anal. Calcd for $C_{109}H_{154}Br_2O_{24}N_2Si_{16}$ (%): C, 52.67; H, 6.24; N, 1.13. Found: C, 52.11; H, 6.21; N, 1.07.

General Procedure for the Synthesis of Alternating Copolymers PFO—POSS. Aqueous potassium carbonate (2 M) and aliquate 336 were added to a solution of the POSS-appended fluorene dibromide monomer **4**, dibromide **5**, and diboronate **6** in toluene. The mixture was degassed and purged with nitrogen three times. The catalyst, tetrakis(triphenylphosphine)palladium (3.0 mol %), was added in one portion under a nitrogen atmosphere. The solution was then heated at 90 °C and vigorously stirred under nitrogen for 5 days. End group capping was performed by heating the solution under reflux for 6 h sequentially with phenylboronic acid and bromobenzene. After cooling, the polymer was recovered by precipitating it into a mixture of methanol and acetone (4:1). The crude polymer was collected, purified twice by reprecipitation from THF into methanol, and subsequently dried under vacuum at 50 °C for 24 h. The ^{1}H and ^{13}C NMR spectra of **PFO** and **PFO—POSS** appear to be identical because of the low content of **POSS** in the latter polymer.

Characterization. ^{1}H, ^{13}C, and ^{29}Si nuclear magnetic resonance (NMR) spectra of the compounds were obtained using a Bruker DRX 300 MHz spectrometer. Mass spectra of the samples were obtained on a JEOL JMS-SX 102A spectrometer. Fourier transform infrared (FTIR) spectra of the synthesized materials were acquired using a Nicolet 360 FT-IR spectrometer. Gel permeation chromatographic analyses were performed on a Waters 410 Differential refractometer and a Waters 600 controller (Waters Styragel column). All GPC analyses of polymers in THF solutions were performed at a flow rate of 1 mL/min at 40 °C; the samples were calibrated using polystyrene standards. Thermogravimetric analysis (TGA) and differential scanning calorimetry (DSC) measurements were performed under a nitrogen atmosphere at heating rates of 20 and 10 °C/min, respectively, using Du Pont TGA-2950 and TA-2000 instruments, respectively. UV−vis absorption and photoluminescence (PL) spectra were recorded on a HP 8453 spectrophotometer and a Hitachi F-4500 luminescence spectrometer, respectively. Before investigating the thermal stability of the synthesized polymers, their polymer films were annealed in air at 200 °C for 2 h.

Device Fabrication and Testing. The electroluminescent (EL) devices were fabricated on an ITO-coated glass substrate that was precleaned and then treated with oxygen plasma before use. A layer of poly(ethylene dioxythiophene):poly(styrenesulfonate) (PEDOT:PSS, Baytron P from Bayer Co.; ca. 40 nm thick) was formed by spin-coating from its aqueous solution (1.3 wt %). The EL layer was spin-coated at 1500 rpm from the corresponding toluene solution (15 mg mL^{-1}) on top of the vacuum-dried PEDOT:PSS layer. The nominal thickness of the EL layer was 65 nm. Using a base pressure below 1 × 10^{-6} Torr, a layer of Ca (30 nm) was vacuum deposited as the cathode and a thick layer of Al was deposited subsequently as the protecting layer. The current−voltage characteristics were measured using a Hewlett-Packard 4155B semiconductor parameter analyzer. The power of the EL emission was measured using a Newport 2835-C multifunction optical meter. The brightness was calculated using the forward output power

Scheme 2. Synthesis of PFO−POSS Copolymers

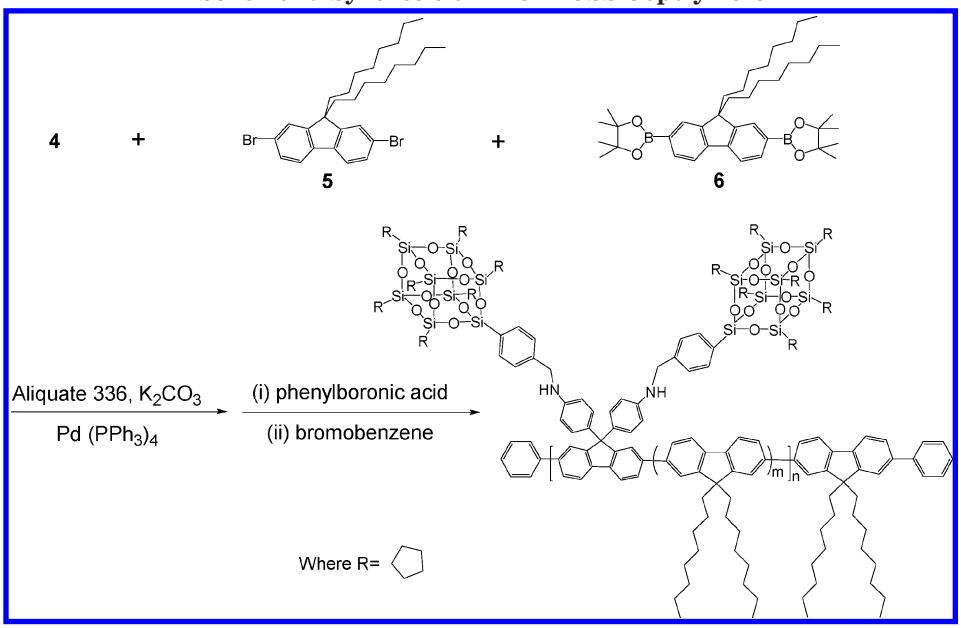

and the EL spectra of the devices; a Lambertian distribution of the EL emission was assumed.

Results and Discussion

Figure 1 displays the ^{1}H NMR spectra of 9,9′-bis(4-aminophenyl)-2,7-dibromofluorene (**3**), **Cl—POSS**, and **D-POSS—diAF** (**4**). The peak for the NH protons shifted downfield from 3.59 ppm for **3** to 4.48 ppm for **4**, while the CH_2 peak of **Cl—POSS** shifted upfield from 4.47 to 4.21 ppm in **D-POSS—diAF**. The ratio of the peak areas of the benzylic CH_2 and NH protons is ca. 2:1. Taken together, all of these data suggest that **Cl—POSS** had reacted with 4-aminophenyl fluorene to form **D-POSS—diAF**. Table 1 lists the thermal properties and molecular weight distributions of the **PFO—POSS** copolymers. Both the thermal degradation and glass transition temperature increased as the amount of **POSS** in **PFO** increased, presumably because the tethered **POSS** enhanced the thermal stability and retarded the polymer chain mobility. The molecular weights of the **PFO—POSS** copolymers decreased upon increasing the **POSS** content; this phenomenon can be attributed to the steric hindrance caused by **POSS** during the polymerization process.

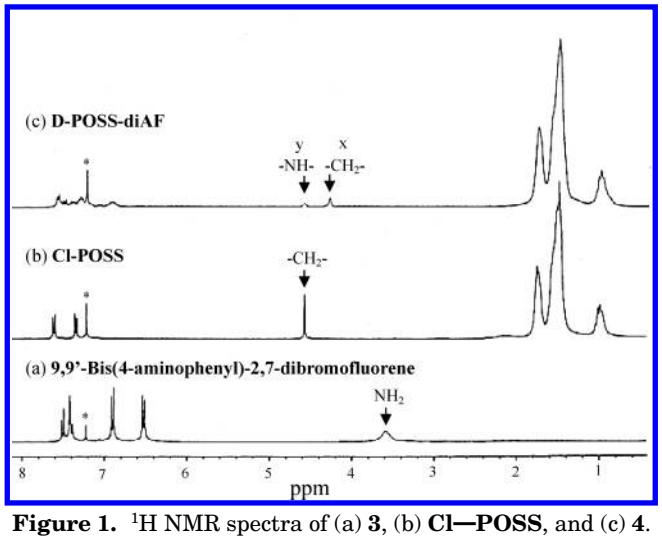

Figure 1. ^{1}H NMR spectra of (a) **3**, (b) **Cl—POSS**, and (c) **4**.

Table 1. Physical Properties of the PFO−POSS Copolymers

	T_d[a] (°C)	M_n	M_w	PDI	yield (%)
PFO	372	27000	51000	1.86	96
PFO—POSS-1%	382	21000	42000	1.96	78
PFO—POSS-3%	381	20000	37000	1.85	68
PFO—POSS-5%	397	16000	31000	1.93	79
PFO—POSS-10%	416	12000	24000	1.97	65

[a] Temperature at which 5% weight loss occurred, based on the initial weight.

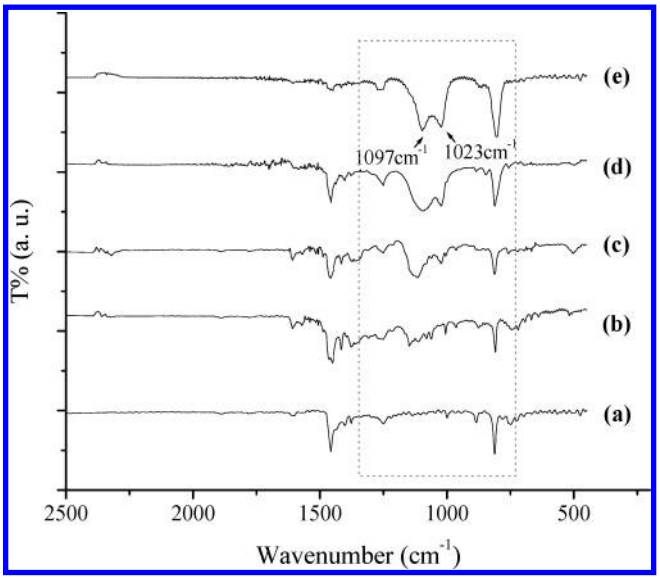

Figure 2. FTIR spectra of (a) **PFO**, (b) **PFO—POSS-1%**, (c) **PFO—POSS-3%**, (d) **PFO—POSS-5%**, and (e) **PFO—POSS-10%**.

Figure 2 displays FTIR spectra of **PFO** copolymers containing different amounts of **POSS**. The FTIR spectrum of **POSS** displays two major characteristic peaks in the range 1000−1180 cm^{-1} (Si−O−Si stretching). The Si−C band at 1074 cm^{-1}, however, overlaps with the Si−O−Si band and, thus, could not be observed clearly.

Figure 3 displays the X-ray diffraction curves of **Cl—POSS**, **PFO**, and **PFO—POSS**. We observed no

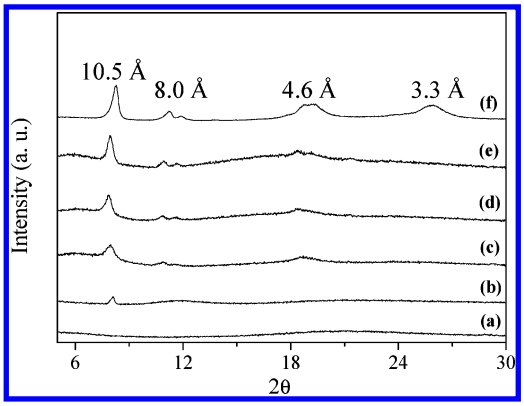

Figure 3. X-ray diffraction curves of **PFO—POSS** nanocomposite films: (a) **PFO**, (b) **PFO—POSS-1%**, (c) **PFO—POSS-3%**, (d) **PFO—POSS-5%**, (e) **PFO—POSS-10%**, and (f) pure **Cl—POSS**.

Table 2. Optical Properties of the PFO−POSS Nanocomposites

	λ_{max} (UV, nm)		λ_{max} (PL, nm)[a]		quantum yield
	solution[b]	film	solution[b]	film	film[c]
PFO	384	390	418 (441)	425 (448)	0.55
PFO—POSS-1%	374	383	417 (440)	423 (447)	0.57
PFO—POSS-3%	374	381	417 (437)	423 (447)	0.64
PFO—POSS-5%	372	381	417 (437)	423 (447)	0.67
PFO—POSS-10%	362	380	416 (436)	422 (446)	0.86

[a] The data in parentheses are the wavelengths of shoulders and subpeaks. [b] The absorption and emission measured in THF. [c] PL quantum yield estimated relative to a sample of poly(2,7-(9,9′-dioctylfluorene)) ($\Phi_{FL} = 0.55$).

X-ray diffraction peaks for pure **PFO**. There are three distinct diffraction peaks at $2\theta = 8.3$, 19.1, and 26.1° observed for **Cl—POSS** (Figure 3f), which correspond to *d*-spacings of 10.5, 4.6, and 3.3 Å, respectively. The *d*-spacing of 10.5 Å reflects the size of the **Cl—POSS** molecules; the other two spacings reflect the rhombohedral crystal structure of **POSS** molecules.[28] The presence of a small crystal peak of **POSS** in **PFO** indicates a mild degree of aggregation of **POSS** molecules. The DSC curves of pure **PFO**[24] indicate a value of T_g of 62 °C, a crystallization exothermal peak (T_c) at 98 °C, and a melting endothermal peak (T_m) at 155 °C (see the Supporting Information). Only a small T_m at 166 °C appears in the curve for **PFO—POSS-10%**; the disappearance of the T_g and T_c peaks in this case (**PFO** containing 10% **POSS**) can be explained by the fact that the mobility of the **PFO** main chains, including chain folding, is severely retarded by the steric hindrance imposed by the bulky side-chain-tethered **POSS** units, as has been reported in the literature.[25] The UV−vis and photoluminescence spectra of **PFO** and **PFO-POSS** recorded in THF are presented in the Supporting Information. Table 2 lists the wavelengths of the absorption and PL maxima and the quantum yields of **PFO—POSS**. The absorption and emission peak maxima of **PFO** occur at 384 and 418 nm, respectively; these values are close to those reported in the literature.[26] We observed no aggregation band in these spectra because THF is a good solvent for **PFO**. The absorption and emission peaks for **PFO** and **PFO—POSS** are almost identical. For each polymer, the absorption peak maximum in solution (THF) is located between 384 and 362 nm, with a slight blue shift caused by the presence of **POSS**; the PL maxima occur at similar wavelengths for all of the polymers. The quantum yields of the

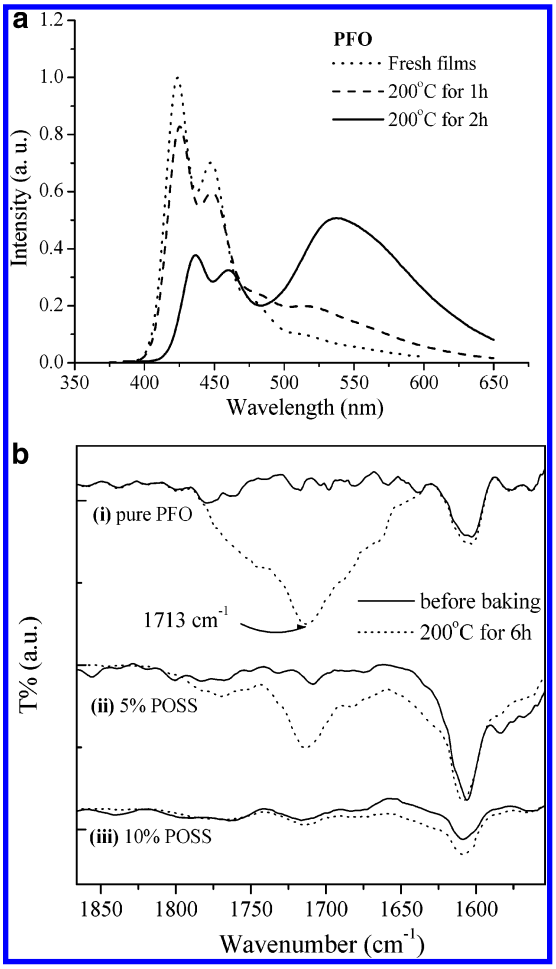

Figure 4. (a) PL spectra of **PFO** films before annealing (dotted line) and after annealing at 200 °C for 1 h (dashed line) and 2 h (solid line) under a nitrogen atmosphere. (b) FTIR spectra of (i) **PFO**, (ii) **PFO—POSS-5%**, and (iii) **PFO—POSS-10%** before (solid line) and after (dashed line) baking at 200 °C for 6 h.

PFO—POSS copolymers increased substantially as the amount of tethered **POSS** increased. In particular, the quantum yield of **PFO** containing 10% **POSS** was 54% higher than that of pure **PFO** (0.86 vs 0.55). This finding can be attributed to the steric hindrance caused by the **POSS** units preventing aggregation of the **PFO** main chains, which, in turn, reduces the degree of dimer formation after excitation. This phenomenon is a result of the particular side-chain-tethered **POSS** architecture that we have employed: it has not been reported in previous studies of **POSS/PFO** copolymers. The other significant effect that the incorporation of the silsesquioxane into **PFO** side chain causes is the persistence of luminescence behavior after thermal treatment of **PFO—POSS**. The stability of both color and luminescence at elevated temperatures are critical for polymer LEDs because sometimes the operating temperature of these devices exceeds 86 °C. Next, we investigated in detail the effect that thermal treatment has on **POSS**-incorporated **PFO**. Figure 4a displays the photoluminescence spectra of **PFO** as a solid film after heat treatment at 200 °C; in all cases, the absorption peaks at 386 nm remain. Other than the main peak at 425 nm, we observe an additional small peak, at ca. 530 nm, in the spectrum of **PFO** film exposed at 200 °C for 1 h. The green emission peak at 530 nm increased in intensity, while the intensity of the main 425 nm peak

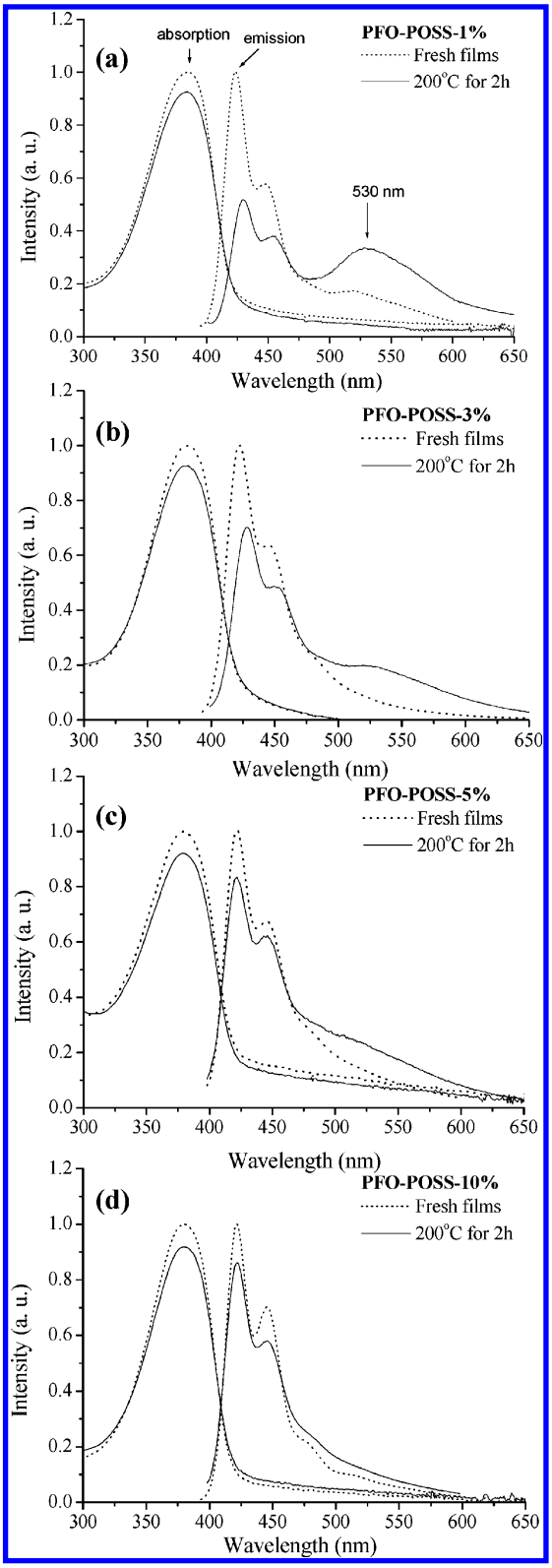

Figure 5. UV−vis absorption and PL spectra of (a) **PFO—POSS-1%**, (b) **PFO—POSS-3%**, (c) **PFO—POSS-5%**, and (d) **PFO—POSS-10%** films before (dotted line) and after (solid line) annealing at 200 °C for 2 h under a nitrogen atmosphere.

reduced quite dramatically, after annealing the **PFO** film for 2 h. Figure 4b indicates that, after thermal treatment, the intensity of the keto peak (C=O, 1713 cm^{-1}) in the FTIR spectra decreases as the amount of **POSS** in **PFO** increases: almost no keto peak appears

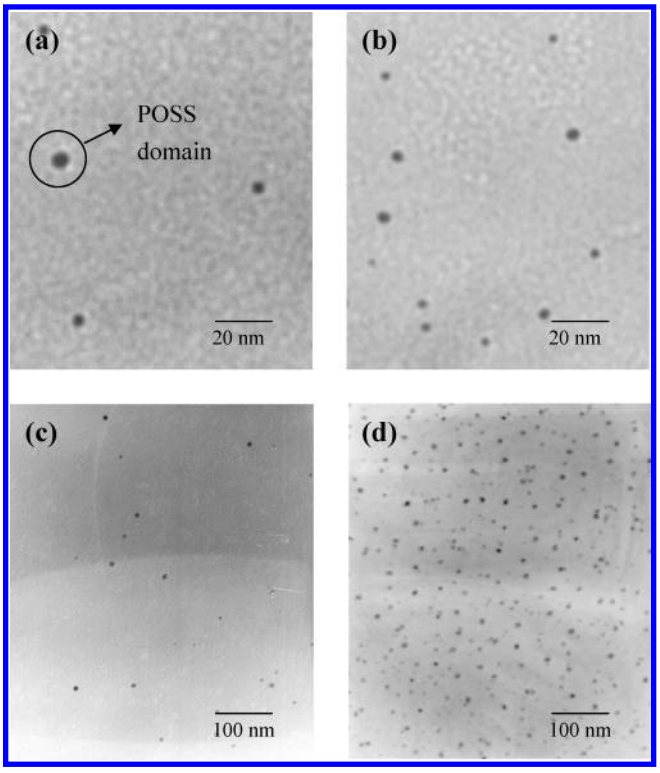

Figure 6. Transmission electron micrographs of (a) **PFO—POSS-1%**, (b) **PFO—POSS-3%**, (c) **PFO—POSS-5%**, and (d) **PFO—POSS-10%**.

in the spectrum of the sample containing 10% **POSS**. Undesired fluorescence emission resulting from the oxidation defects in polymer chains can be reduced by improving the thermal-oxidation properties of the polymers.[18b,28] In this case, the bulky siloxane units attached to 4-aminophenyl spacer appear to provide a good shield for the neighboring dialkyl groups from thermal oxidation because the thermal degradation temperature of siloxane units is higher than that of dialkyl chains, as evidenced in the TGA results of **POSS/PFO** copolymer in Table 1, where the thermal degradation temperature of the copolymer increases with the amount of **POSS**.

Figure 5 presents the normalized absorption and PL emission spectra of the annealed **PFO—POSS** films with respect to that of their fresh films. The fact that the absorption λ_{max} of **PFO—POSS** in Figure 5, parts c and d appears at the same wavelength before and after heating suggests that the thermal treatment did not disrupt the conjugation in these **PFO—POSS** samples. The PL spectrum of **PFO** containing 1% **POSS** exhibits a much smaller shoulder at 530 nm than that for the pure **PFO** after the same thermal treatment. This peak was reduced further when 3% **POSS** (Figure 5b) was present and became an insignificant shoulder at ca. 500 nm when ≥5% **POSS** was incorporated into **PFO** (Figure 5c,d). These results suggest that the tethered **POSS** units not only reduced the aggregation of **PFO** molecular chains but also prevented keto defects from forming upon thermal treatment. Figure 6 presents transmission electron microscopy (TEM) images of different **PFO—POSS** samples; these images clearly reveal that no large aggregates have formed, but small domains of **POSS** are present, and the **POSS** domains are dispersed well in the polymer matrix.

Electroluminescence (EL) Characteristics. Figure 7 displays the electroluminescence (EL) spectra of

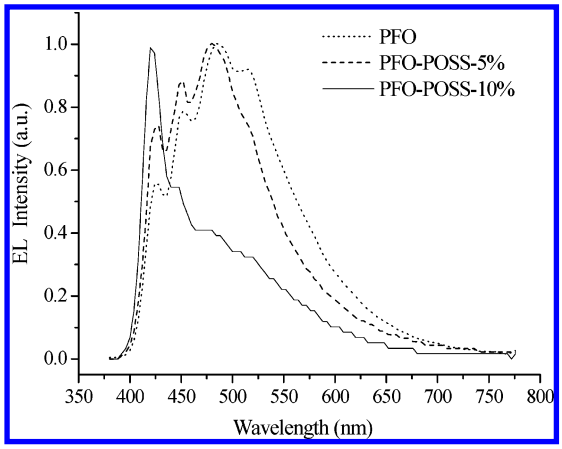

Figure 7. Electroluminescence spectra of the devices prepared from **PFO—POSS** and **PFO** in the configuration ITO/PEDOT/polymer/Ca/Al.

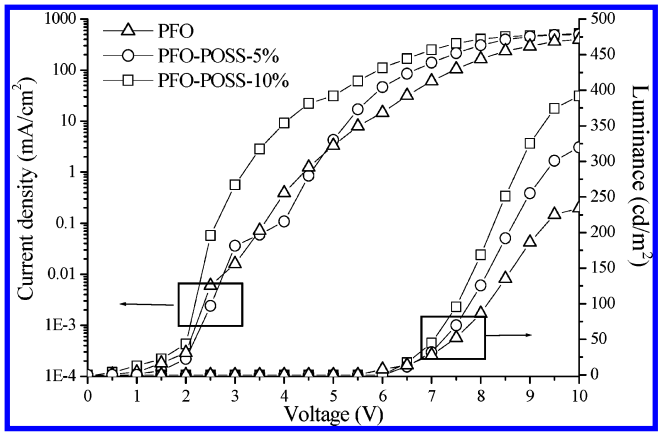

Figure 8. *I*−*V* curves of the devices prepared from **PFO—POSS** and **PFO** in the configuration ITO/PEDOT/polymer/Ca/Al.

PFO—POSS devices. The EL device prepared from **PFO** emits a weak blue signal at 425 nm and a more intense green signal in the range 470−600 nm, which is presumably due to the aggregation and keto defects discussed previously. When 5% **POSS** was included in **PFO**, the intensity of the peak at 425 nm increased, but the intensity of the green emission remained approximately the same. In the case where 10% **POSS** was incorporated in **PFO**, the green emission in the range 470−600 nm was reduced sharply, while the peak at 425 nm became the major emission peak and had an intensity much larger than that exhibited by the device prepared from pure **PFO**. The reduction in the green emission is apparently due to the presence of the siloxane units. The introduction of bulky siloxane units into polyfluorene side chain presumably serves a dual function; it not only hinders oxidation of fluorenes but also increases the interchain distance, thereby retarding the interchain interactions and leading to a reduction of excitons migration to defect sites as discussed in a previous study.[27]

Figure 8 displays the variations of the current density and brightness of the EL devices. The turn-on voltage increased to 5.8 V for**PFO** containing 10% **POSS** from 5.4 V for the pure-**PFO** EL device. A significant increase (68%) in the maximum brightness of the **PFO—POSS-10%**-based device occurred relative to that of the pure-**PFO** EL device (392 vs 234 cd/m^2) at a drive voltage of 10 V and a current density of 576 mA/cm^2. These improvements might be due to a combination of a lesser degree of aggregation and fewer keto defects being formed upon the incorporation of **POSS** into **PFO**.

Summary

We have synthesized a novel polyfluorene side-chain-tethered polyhedral silsesquioxane that has a well-defined architecture. This particular molecular architecture of **PFO—POSS** increases the quantum yield of polyfluorene significantly by reducing the degree of interchain aggregation; it also results in a purer and stronger blue light being emitted from the EL device by preventing the formation of keto defects.

Acknowledgment. The authors thank the National Science Council, Taiwan, and the US Air Force Office of Scientific Research for funding this work through Grants NSC 91-2120-M-009-001 and AOARD-03-4018, respectively. Mr. Yao-Te Chang is also acknowledged for experimental assistance and helpful discussions.

Supporting Information Available: Figures showing normalized UV−vis absorption, photoluminescence spectra, DSC, and TGA of **PFO** and **PFO—POSS**. This material is available free of charge via the Internet at http://pubs.acs.org.

References and Notes

(1) (a) Greenham, N. C.; Moratti, S. C.; Bradley, D. D. C.; Friend, R. H.; Holmes, A. B. *Nature* **1993**, *365*, 628. (b) Gustafsson, G.; Cao, Y.; Treacy, G. M.; Klavetter, F.; Colaneri, N.; Heeger, A. J. *Nature* **1992**, *357*, 477. (c) Burroughes, J. H.; Bradley, D. D. C.; Brown, A. R.; Marks, R. N.; Mackay, K.; Friend, R. H.; Burns, P. L.; Holmes, A. B. *Nature* **1990**, *347*, 539. (d) Jenekhe, S. A.; Osaheni, J. A. *Science* **1994**, *620*, 765.

(2) (a) Halls, J. J. M.; Walsh, C. A.; Greenham, N. C.; Marseglia, E. A.; Friend, R. H.; Moratti, S. C.; Holmes, A. B. *Nature (London)* **1995**, *376*, 498. (b) Yu, G.; Gao, J.; Hummelen, J. C.; Wudl, F.; Heeger, A. J. *Science* **1995**, *270*, 1789. (c) Granström, M.; Petritsch, K.; Arias, A. C.; Lux, A.; Andersson, M. R.; Friend, R. H. *Nature* **1998**, *395*, 257.

(3) (a) Yang, Y.; Heeger, A. J. *Nature* **1994**, *372*, 344. (b) Brown, A. R.; Pomp, A.; Hart, C. M.; de Leeuw, D. M. *Science* **1995**, *270*, 972. (c) Sirringhaus, H.; Tessler, N.; Friend, R. H. *Science* **1998**, *280*, 1741. (d) Sirringhaus, H.; Brown, P. J.; Friend, R. H.; Nielsen, M. M.; Bechgaard, K.; Langeveld-Voss, B. M. W.; Spiering, A. J. H.; Janssen, R. A. J.; Meijer, E. W.; Herwig, P.; de Leeuw, D. M. *Nature* **1999**, *401*, 685. (e) Babel, A.; Jenekhe, S. A. *J. Am. Chem. Soc.* **2003**, *125*, 13656.

(4) Ranger, M.; Rondeau, D.; Leclerc, M. *Macromolecules* **1997**, *30*, 7686.

(5) Yu, W.-L.; Pei, J.; Cao, Y.; Huang, W.; Heeger, A. J. *Chem. Commun.* **1999**, 1837.

(6) Pei, J.; Yu, W.-L.; Huang, W.; Heeger, A. J. *Chem. Commun.* **2000**, 1631.

(7) Ego, C.; Marsitzky, D.; Becker, S.; Zhang, J.; Grimsdale, A. C.; Müllen, K.; MacKenzie, J. D.; Silva, C.; Friend, R. H. *J. Am. Chem. Soc.* **2003**, *125*, 437.

(8) (a) Lee, J. I.; Klärner, G.; Miller, R. D. *Chem. Mater.* **1999**, *11*, 1083. (b) Klärner, G.; Lee, J. I.; Davey, M. H.; Miller, R. D. *Adv. Mater.* **1999**, *11*, 115.

(9) (a) Yu, W.-L.; Pei, J.; Huang, W.; Heeger, A. J. *Adv. Mater.* **2000**, *12*, 828. (b) Zeng, G.; Yu, W.-L.; Chua, S.-J.; Huang, W. *Macromolecules* **2002**, *35*, 6907.

(10) Setayesh, S.; Grimsdale, A. C.; Weil, T.; Enkelmann, V.; Müllen, K.; Meghdadi, F.; List, E. J. W.; Leising, G. *J. Am. Chem. Soc.* **2001**, *123*, 946.

(11) (a) Kreyenschmidt, M.; Klärner, G.; Fuhrer, T.; Ashenhurst, J.; Karg, S.; Chen, W. D.; Lee, V. Y.; Scott, J. C.; Miller, R. D. *Macromolecules* **1998**, *31*, 1099. (b) Klärner, G.; Lee, J. I.; Lee, V. Y.; Chan, E.; Chen, J. P.; Nelson, A.; Markiewicz, D.; Siemens, R.; Scott, J. C.; Miller, R. D. *Chem. Mater.* **1999**, *11*, 1800. (c) Lee, J. I.; Klärner, G.; Miller, R. D. *Chem. Mater.* **1999**, *11*, 1083.

(12) (a) Marsitzky, D.; Klapper, M.; Mullen, K. *Macromolecules* **1999**, *32*, 8685. (b) Marsitzky, D.; Murray, J.; Scott, J. C.; Carter, K. R. *Chem. Mater.* **2001**, *13*, 4285. (c) Marsitzky, D.; Vestberg, R.; Blainey, P.; Tang, B. T.; Hawker, C. J.;

Carter, K. R. *J. Am. Chem. Soc.* **2001**, *123*, 6965. (d) Setayesh, S.; Grimsdale, A. C.; Weil, T.; Enkelmann, V.; Müllen, K.; Meghdadi, F.; List, E. J. W.; Leising, G. *J. Am. Chem. Soc.* **2001**, *123*, 946. (e) Ego, C.; Grimsdale, A. C.; Uckert, F.; Yu, G.; Srdanov, G.; Müllen, K. *Adv. Mater.* **2002**, *14*, 809. (f) Pogantsch, A.; Wenzl, F. P.; List, E. J. W.; Leising, G.; Grimsdale, A. C.; Müllen, K. *Adv. Mater.* **2002**, *14*, 1061. (g) Lupton, J. M.; Schouwink, P.; Keivanidis, P. E.; Grimsdale, A. C.; Müllen, K. *Adv. Funct. Mater.* **2003**, *13*, 154.

(13) Shu, C. F.; Dodda, R.; Wu, F. I.; Liu, M. S.; Jen, A. K. Y. *Macromolecules* **2003**, *36*, 6698.

(14) Zeng, G.; Yu, W. L.; Chua, S. J.; Huang, W. *Macromolecules* **2002**, *35*, 6907.

(15) Xiao, S.; Nguyen, M.; Gong, X.; Cao, Y.; Wu, H.; Moses, D.; Heeger, A. J. *Adv. Funct. Mater.* **2003**, *13*, 25.

(16) (a) Cho, H. J.; Jung, B. J.; Cho, N. S.; Lee, J.; Shim, H. K. *Macromolecules* **2003**, *36*, 6704. (b) Lim, E.; Jung, B. J.; Shim, H. K. *Macromolecules* **2003**, *36*, 4288.

(17) Kulkarni, A. P.; Jenekhe, S. A. *Macromolecules* **2003**, *36*, 5285.

(18) (a) List, E. J. W.; Guentner, R.; Freitas, P. S.; Scherf, U. *Adv. Mater.* **2002**, *14*, 374. (b) Romaner, L.; Pogantsch, A.; Freitas, P. S.; Scherf, U.; Gaal, M.; Zojer, E.; List, J. W. *Adv. Funct. Mater.* **2003**, *13*, 597. (c) Kulkarni, A. P.; Kong, X.; Jenekhe, S. A. *J. Phys. Chem. B*. **2004**, 108, 8689. (d) Cho, H. J.; Jung, B. J.; Cho, N. S.; Lee, J.; Shim, H. K. *Macromolecules* **2003**, *36*, 6704. (e) Lin, W. J.; Chen, W. C.; Wu, W. C.; Niu, Y. H.; Jen, A. K. Y. *Macromolecules* **2004**, *37*, 2335.

(19) (a) Leu, C. M.; Chang, Y. T.; Wei, K. H. *Macromolecules* **2003**, *36*, 9122. (b) Kraft, A.; Grimsdale, A. C.; Holmes, A. B. *Angew. Chem., Int. Ed. Engl.* **1998**, *37*, 402.

(20) Setayesh, S.; Grimsdale, A. C.; Weil, T.; Enkelmann, V.; Müllen, K.; Meghdadi, F.; List, E. J. W.; Leising, G. *J. Am. Chem. Soc.* **2001**, *123*, 946.

(21) Miller, T. M.; Neenan, T. X.; Zayas, R.; Bair, H. E. *J. Am. Chem. Soc.* **1992**, *114*, 1018.

(22) Ranger, M.; Leclerc, M. *Macromolecules* **1999**, *32*, 3306.

(23) Leu, C. M.; Chang, Y. T.; Wei, K. H. *Chem. Mater.* **2003**, *15*, 3721.

(24) Grell, M.; Bradley, D. D. C.; Inbasekaran, M.; Woo, E. P. *Adv. Mater.* **1997**, *9*, 798.

(25) Wu, F. I.; Reddy, D. S.; Shu, C. F.; Liu, M. S.; Jen, A. K. Y. *Chem. Mater.* **2003**, *15*, 269.

(26) (a) Grell, M.; Bradley, D. D. C.; Long, X.; Chamberlain, T.; Inbasekaran, M.; Woo, E. P.; Soliman, M. *Acta Polym.* **1998**, *49*, 439. (b) Grice, A. W.; Bradley, D. D. C.; Bernius, M. T.; Inbasekaran, M.; Wu, W. W.; Woo, E. P. *Appl. Phys. Lett.* **1998**, *73*, 629. (c) Friend, R. H.; Gymer, R. W.; Holmes, A. B.; Burroughes, J. H.; Marks, R. N.; Taliani, C.; Bradley, D. D. C.; Dos Santos, D. A.; Bredas, J. L.; Logdlund, M.; Salaneck, W. R. *Nature* **1999**, *397*, 121.

(27) Grimsdale, A. C.; Leclère, P.; Lazzaroni, R.; MacKenzie, J. D.; Murphy, C.; Setayesh, S.; Silva, C.; Friend, R. H.; Müllen, K. *Adv. Funct. Mater.* **2002**, *12*, 729.

(28) Zheng, L.; Waddon, A. J.; Farris, R. J.; Coughlin, E. B. *Macromolecules* **2002**, *35,* 2375.

MA0479520